Structure and Optical Properties of Nanocrystalline Titanium Dioxide Prepared via Pulsed Laser Ablation in Liquid

Elena D. Fakhrutdinova, Antonina V. Palatova, Valery A. Svetlichnyi
Siberian Physical-Technical Institute of Tomsk State University, Tomsk, Russia

***Abstract* – Crystal structure and optical properties of titanium dioxide prepared via pulsed laser ablation of metallic Ti in water were investigated. The ultrafine powder obtained after drying the ablated dispersion consisted of dark blue nanocrystalline TiO_2 containing anatase and rutile phases with an average particle size of 5-10 nm. This material exhibited an intense additional absorption in the visible region, which is associated with the presence of a large number of defect states, namely different types of oxygen vacancies. The effect of heat treatment on the structural and optical properties of TiO_2 was studied.**

***Index Terms* – titanium dioxide, defect state, photoluminescence.**

I. INTRODUCTION

RESENTLY, OXIDE SEMICONDUCTOR nanomaterials showing unique properties attract attention of researchers. Among these materials, nanocrystalline titanium dioxide (TiO_2) can be distinguished. Due to its optical properties and chemical resistance, this wide-gap semiconductor has a sufficiently high refractive index (2.5-2.7) and is used as a white pigment in the manufacture of paints, coatings, plastics, paper, inks, sunscreens, foodstuffs, and most toothpastes [1, 2].

TiO_2 has a high photoactivity due to the relatively long lifetime of photogenerated charge carriers (~ 250 ns), good photo-stability and environmental safety. That makes this material promising for use in photovoltaics, in gas and moisture sensors, in water purification, self-cleaning of various surfaces, for example, glasses, photochemical cells, protective and functional coatings on optical elements [3]. One of the limitations of titanium dioxide using as an optically active material, is the large width of the bandgap, which implies only UV radiation for its photoexcitation. Therefore, obtaining materials based on titanium dioxide sensitized to low energy photons (visible radiation) without losing its activity is one of the priority aims.

The literature data shows that the optical properties of titanium dioxide significantly depend on the method of its preparation and purification, the presence of dopant impurities and defects, the surface state and its subsequent treatments [4]. At present, there are active efforts applied to develop new technologies for synthesis of materials based on titanium dioxide that would absorb in the visible range. Technologies of sol-gel synthesis are widespread [5,6]. Physical methods of synthesis are also of great interest, for instance the pulsed laser ablation (PLA) method [7-9]. The processes occurring during PLA are high-energy, which leads to the production of a substance in a highly dispersed and highly defective state, which certainly affects its physical-chemical and optical properties.

II. PROBLEM DEFINITION

The spectral absorption region of titanium dioxide is usually expanded by doping and co-doping with cations and anions of metals and non-metals, and also by modifiers addition witch absorb in the visible range of spectrum [10].

Pulsed laser ablation of metallic titanium in water allows preparation of “pure” nanocrystalline titania without the use of additional precursors. This TiO_2 is in a highly defect state, and absorb in the visible range. The main objective of this study is to identify the nature of the defect states that increase the absorption in the visible region, as well as to study the effect of heat treatment on the structure of TiO_2 and its optical properties.

IV. EXPERIMENTAL SETUP

Nanocrystalline TiO_2 powders were synthesized in two stages. At the first stage, the colloidal solution was produced by pulsed laser ablation method of bulk targets in water. At the second stage, the colloidal solution was dried.

Basic harmonic of the Nd:YAG laser (LOTIS TII, model LS2131M-20) was used for PLA, with wavelength of 1064 nm and pulse energy up to 180 mJ. Pulse duration and pulse frequency were 7 ns and 20 Hz respectively.

Metal Ti plate (99.9% pure) with dimensions of 10×25×1 mm was used as a target. In order to ensure uniform irradiation and prevent the emergence of craters on the surface, the target was automatically moved in the *XY* plane orthogonal to the laser beam by two linear stepper motor translation stages (Standa, model 8MT173-50). The concentration of particles in the dispersion was controlled on the basis of target mass loss. The setup for PLA in a liquid is described in details in [11].

978-1-5386-5021-9/18/$31.00 ©2018 IEEE

The colloidal solution produced was dried in the air in open glass vessels at the temperature not exceeding 60°C. As a result, 3 grams of nanocrystalline powder were prepared and used in further research. Some of the samples were annealed in the muffle chamber at temperatures from 200 to 1000°C. The following identifiers were assigned to the samples produced: TiO_2; TiO_2 200; TiO_2 400; TiO_2 600; TiO_2 800; TiO_2 1000, respectively. For comparison P25 Degussa nanocrystalline titanium dioxide powder was used.

The size and shape of the particles produced was examined using the transmission electron microscope Phillips CM 12.

The crystalline structure was studied by method of X-ray diffraction (XRD) using Shimadzu XRD 6000 diffractometer. The phase compositions were identified relying on the PDF4 database. Distribution of percentage content across phases in the sample was calculated using PowderCell 2.4 software complex.

Optical properties of nanocrystalline powders were examined by diffuse reflectance spectroscopy (DRS) on Cary spectrophotometer with accessory DRA-CA-30I, Labsphere in the wavelength range of 200-800 nm. MgO was used as a measurement standard. Band gap was calculated from diffuse reflectance spectra based on absorption edge of the material [12]. The data obtained by DRS were presented in the form of Kubelka-Munk function:

$$F(R) = (1-R)^2 / 2R .$$

Then the graphical dependence was drawn:

$$\alpha^{1/2} = f(h\nu),$$

$$\alpha = E_{h\nu} \cdot (1-R)^2 / 2R .$$

The linear segment of absorption edge was extrapolated on axis X and intersection point of the tangent line and the axis corresponded to the bandgap.

Defect structure of the powders was studied based on photoluminescence spectra using Renishaw inVia Raman microscope, UK. The emission spectra were registered upon excitation by laser radiation with λ = 405 nm and a diffraction grating of 2400 lines/mm in the range of 200-740 nm.

IV. DISCUSSION OF RESULTS

The titanium dioxide initial sample is a dark blue powder, which after the heat treatment at 200 and 400°C changes its color to light gray. After annealing at 600°C it becomes white powder; at 800°C and 1000°C it becomes light yellow.

Transmission electron microscopy (TEM) image of the TiO_2 sample is shown in Fig. 1. The material consists of fine spherical particles with an average size of 5-10 nm, and an insignificant number of large particles with a size of up to 80 nm also present. Large spherical particles are surrounded by a net of smaller agglomerated particles.

The metallic titanium target initially had a hexagonal crystalline structure with symmetry space group P63/mmc. After metal target ablation process the titania is amorphous. After the heat treatment at 200°C the sample remains amorphous, but it exhibits seeds of crystalline anatase (tetragonal structure with space symmetry group I4/amd) and rutile (tetragonal structure with space symmetry group P42/mnm).

After annealing at 400 and 600°C the anatase and rutile phases remain, and the amorphous phase does not appear in the X-ray patterns (Fig. 2). Moreover, after annealing at 600ºC the anatase is the dominated phase - 62%, and only 38% of the rutile phase presents. Also, at the temperature increasing the intensity of the lines increases, and the half-width of the X-ray bonds decreases.

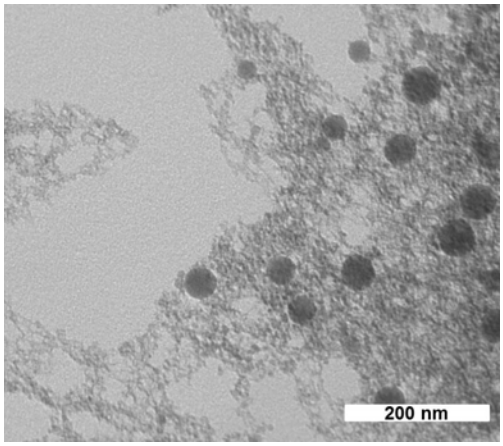

Fig.1. TEM image of TiO_2

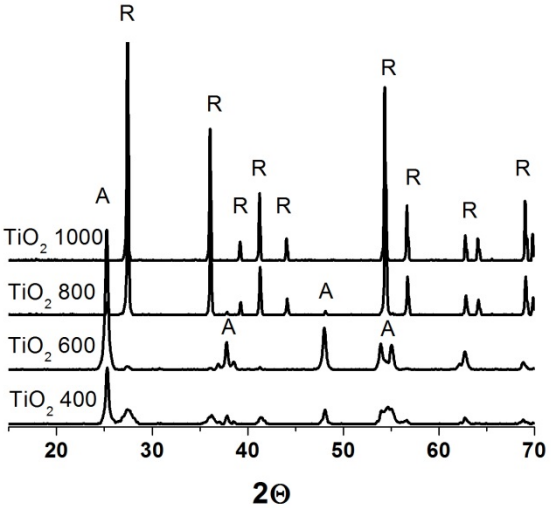

Fig.2. XRD pattern of TiO_2 after annealing

This can relate to the enlargement of the particles, and reduction of the defect states number in the nanoparticles surface layers. After annealing at a higher temperature the anatase phase begins transforming into the rutile, and at 1000°C the sample consists entirely of the rutile phase. The literature data shows that the phase transition of anatase to rutile in titanium dioxide begins at a temperature of 450°C;

and at 750°C a pure rutile phase is formed [13]. However, our studies show that the pulsed laser ablation method makes it possible to obtain more temperature resistant anatase nanoparticles. Such thermal resistance to phase transformations can be explained by the formation of defects in the surface layer of nanoparticles associated with the rapid cooling of substance during laser ablation in a liquid.

In addition to X-ray diffraction, Raman spectroscopy is an effective tool for studying the phase composition. Raman spectra of titanium dioxide are sufficiently well studied [14, 15]. The Raman spectra are shown in Fig. 3. Spectra of nanocrystalline powders are consistent with the general form of the anatase modes [16]. In this case, the anatase phase is also well identified for initial amorphous for XRD samples.

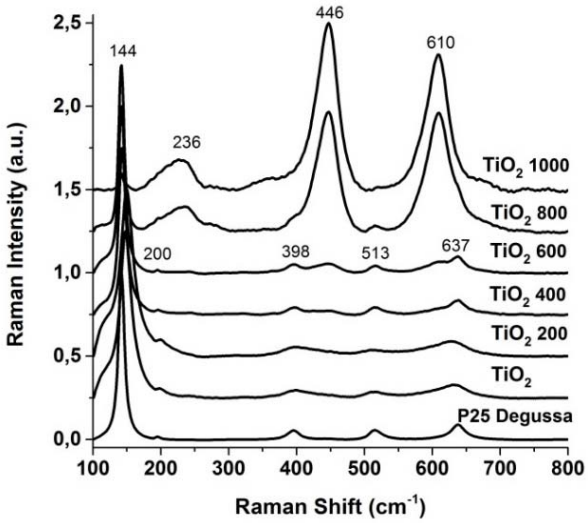

Fig.3. Raman spectra of TiO_2 samples before and after annealing

The most intense band in the 144-146 cm^{-1} region corresponds to the Eg mode; the less intense bands in the region of 200, 398, 513 and 637 cm^{-1} are the Eg, B1g, A1g and Eg modes of the anatase, respectively [15]. Also, the presence of the rutile phase in the Raman spectra of the samples is noticeable, the intensity of rutile modes increases with increasing of the annealing temperature. Modes in the region of 236 (B1g), 446 (Eg), and 610 (A1g) cm^{-1} correspond to rutile [17-18]. After annealing at 800 and 1000 °C the rutile modes dominate in the Raman spectra, that consistent with the XRD data. It should also be noted, that amorphous mods of titanium dioxide in the Raman spectra were not found [19]. The spectrum type of TiO_2 indicates that the sample is in the crystalline form. Comparing the XRD and Raman spectroscopy data, it can be concluded that the initial sample consists of very small crystallites having only a short-range order.

Optical properties of powders were examined by the diffuse reflection method. From ultraviolet-visible (UV-vis) spectra shown in Fig.4 it can be seen that all the samples have additional absorption in the visible range. The initial TiO_2 powder (without annealing) shows most intensive absorption. Differences in the absorption spectra are observed both in the UV range - shifting of the absorption edge, and in the visible range - an increase in absorption. The shifting of the absorption edge for TiO_2 800 and TiO_2 1000 samples is related to the anatase/rutile phase transition, and the predominance of the rutile phase in the samples. The decrease of the absorption edge is associated with a significant enlargement of the particles during annealing. The increase in absorption in the visible range can be due to both the presence of defect states and the presence of a metallic Ti. However, according to XRD data metal Ti was not found in the sample composition. Consequently, the increase in absorption in the visible region of the spectrum is due to the presence of different nature defective states. The main types of crystal lattice intrinsic defects of TiO_2 are various types of oxygen vacancies (F, F^+ and F^{2+} centers), interstitial Ti^{3+} and Ti^{4+} ions, and also the crystallographic shift planes, whose relative concentration depends on the oxygen defect conditions [20]. It should be noted that after annealing of the samples, the number of defect states in the structure decreases, and additional absorption intense decreases (curves of TiO_2 400 and TiO_2 600 in Fig. 4). On UV-vis spectra of the samples TiO_2 800 and TiO_2 1000, an increase in absorption in visible region can be seen again, and samples become a light yellow. Typically, titanium dioxide in any modification is a white crystal that turns yellow during the heated, and turns white again upon cooling. Therefore, in this case, there is an assumption that during the PLA and high-temperature annealing the crystal lattice is restructured with a change in the number of oxygen atoms. However, this statement requires additional studies.

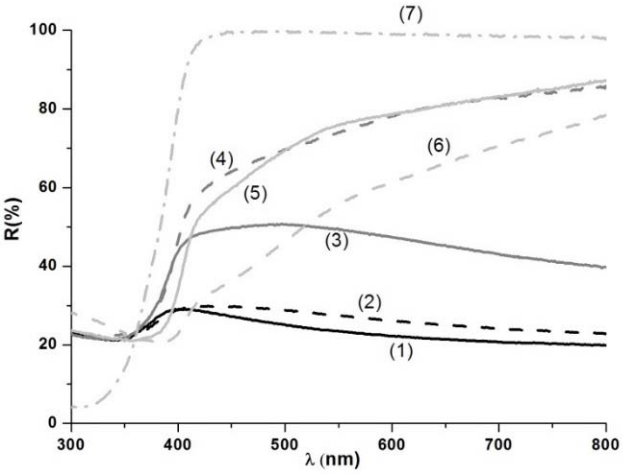

Fig.4. Diffuse reflectance spectra of TiO_2 before and after annealing: (1) TiO_2; (2) TiO_2 200; (3) TiO_2 400; (4) TiO_2 600; (5) TiO_2 800; (6) TiO_2 1000; (7) P25 Degussa.

At the absorption edge of samples, the bandgap were calculated, and its values are presented in Table I. According to the literature data the band gap of the anatase is 3.2 eV and of the rutile – 3.0 eV [11].

TABLE I
VALUES OF BANDGAP AND PARTICLES AVERAGE SIZE

Sample	Bandgap, eV	Particle size, nm
TiO_2	2.88	10
TiO_2 200	2.90	14
TiO_2 400	2.95	14
TiO_2 600	2.96	24
TiO_2 800	2.98	98
$TiO_2$1000	3.05	455

The decrease in the bandgap value for materials prepared via pulsed laser ablation is associated with the presence of a different nature defect states in the bandgap of TiO_2 that lay higher in energy than the 2pO levels forming TiO_2 valence band. Thus, defect levels blur a clear boundary of the valence band, and "narrow" the bandgap. Additional levels existence appears as additional absorption in the visible region of the spectrum. For TiO_2 800 and TiO_2 1000 samples the calculated bandgap coincides with the literature data for the rutile phase.

Photoluminescence (PL) provides more information about the nature of defective states. In Fig. 5 the photoluminescence spectra of materials at the excitation wavelength of 405 nm are presented.

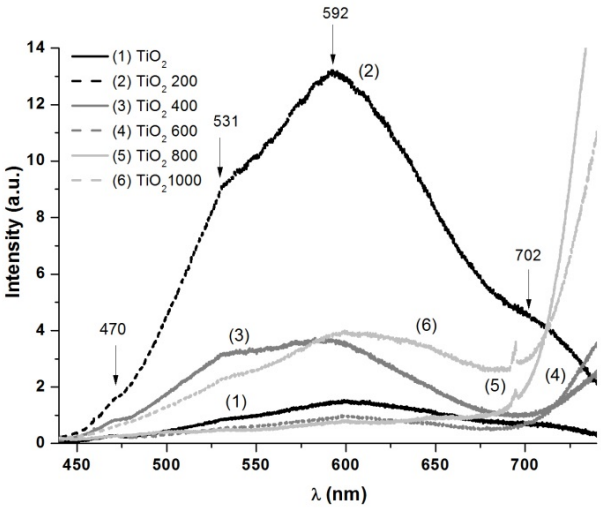

Fig.5. Photoluminescence spectra of TiO_2 before and after annealing

Generally, the interpretation of the photoluminescence spectra of titanium dioxide registered at room temperature is rather complicated, because of the low intensity of PL. However, we succeeded in registering sufficiently intense PL spectra. Analyzing them, we can obtain information on the electronic structure and distribution of electronic states in the samples. All materials presented in Fig. 5, exhibit wide photoluminescence band in the 450-740 nm region. TiO_2 200 sample has the highest photoluminescence intensity. The PL band with a maximum at 470 nm (2.64 eV) belongs to indirect bandgap and surface recombination processes. In addition, this band can also be attributed to excitons localized on TiO_6 octahedra [21]. The photoluminescence band with a maximum at 531 nm (2.33 eV) can be attributed to oxygen vacancies with two trapped electrons, so-called F-centers. The intense band with a maximum at 592 nm (2.09 eV) belongs to the presence of oxygen vacancies with one trapped electron - F^+-center [22]. Also in the region of 600-680 nm it is possible to observe charge carrier transfers associated with defective states in titanium dioxide. These states nature is still under discussion. The PL band with a maximum in the region of 702 nm (1.77 eV) can be attributed to oxygen vacancies with two trapped electrons, that is, to F^{2+}-centers. The centers mentioned above, so-called color centers, usually affect the intensity of photoluminescence [23]. With increasing of oxygen defects number, the number of photo-excited electrons traps on the surface increases. These traps capture photo-induced electrons, and prevent hole-electron recombination. This increases the lifetime of the charge carriers. Note that the narrow peaks appeared in the PL spectra of some samples in the 690 nm region are the overtones of intense Raman modes belonging to rutile (Fig. 3).

After annealing the PL intensity of the samples decreases, which can be correlated with a decrease in the number of defects in TiO_2structure. At the same time, in the infrared range (longer than 700 nm) new bands appear. Their intensity increases with increasing of the annealing temperature. The limitations of the Raman microscope do not allow examination of the photoluminescence in the long-wave region. These studies are planned in the future. Note that the band of long-wavelength photoluminescence correlates with the appearance of additional absorption (yellow color) in samples annealed at 800 and 1000°C.

VI. CONCLUSION

The possibility of preparing a nanocrystalline highly defect titanium dioxide powder by pulsed laser ablation of a bulk metallic Ti target in water and further drying is demonstrated. The initial TiO_2 is a dark blue powder consisted of crystallites with an average size of 5-10 nm. According to XRD data and Raman spectroscopy, the material is nanocrystalline and consists of phases of anatase and rutile. Also it should be noted that this method of preparation allows obtaining nanoparticles with anatase phase more resistant to temperature effects.

Optical properties study show that the material has an intense absorption in the visible region of the spectrum. This additional absorption is due to the presence of defects of various nature in the structure of TiO_2, namely, different types of oxygen vacancies. (F, F^+ and F^{2+}-centers). These F^+ and F^{2+} defect states can act as traps captured photoexcited electrons, that increases the charge carriers lifetime and prevents their recombination. It was found that with an annealing temperature increase, the number of defective states decreases. This affects the absorbtion intensity in the visible region, and also affects the color of the samples.

Thus, the method of pulsed laser ablation allows to obtain nanocrystalline titanium dioxide witch absorb light in the visible range of spectrum. This material can be used in creation of devices for photovoltaics, photochemical cells, coatings on optical elements and for photocatalytic cleaning using the sun as an energy source.

ACKNOWLEDGMENT

This work was conducted as a government task of the Ministry of Education and Science of the Russian Federation, Project Number 3.9604.2017/8.9.

REFERENCES

[1] Zhu X., Chang Y., Chen, Y. Toxicity and bioaccumulation of TiO_2 nanoparticle aggregates in Daphnia magna // Chemosphere, 2010. V. 78. pp. 209-215.

[2] Demetrescu I., Pirvu C., Mitran V., Effect of nano-topographical features of Ti/TiO_2 electrode surface on cell response and electrochemical stability in artificial saliva // Bioelectrochemistry, 2010. V. 79. pp. 122-129.

[3] Fujishima A., Rao T.N., Tryk D.A. Titanium dioxide photocatalysis // J. Photochem. Photobiol. C, 2000. V. 1. pp 1–21.

[4] M.J. Llansola-Portoles, J.J. Bergkamp, Daniel Finkelstein-Shapiro, et al. Controlling Surface Defects and Photophysics in TiO_2 Nanoparticles // J. Phys. Chem. A, 2014. V. 18. pp.10631-10638

[5] Peng T., Zhao D., Dai K., Shi W., Hirao K. Synthesis of titanium dioxide nanoparticles with mesoporous anatase wall and high photocatalytic activity // J. Phys. Chem. B, 2005. V. 109. pp. 4947-4952.

[6] Shabalina A., Fakhrutdinova E., Chen Y-W., Lapin I. Preparation of gold-modified F,N-TiO_2 visible light photocatalysts and their structural features comparative analysis // J. Sol-Gel Sci. Technol, 2015. V. 75. pp. 617-624.

[7] Zeng H., Du X-W., Singh S.C., Kulinich S.A., Yang S., He J., Cai W. Nanomaterials via laser ablation/irradiation in liquid: A review // Adv. Funct. Mater, 2012. V. 22. pp. 1333-1353.

[8] Zimbone M., Buccheri M.A., Cacciato G., Sanz R., Rappazzo G., Boninelli S., Reitano R., Romano L., Privitera V., Grimaldi M.G., Photocatalytical and antibacterial activity of TiO_2 nanoparticles obtained by laser ablation in water, Appl. Catal. B, 2015. V. 165. pp 487-494.

[9] Svetlichnyi V., Shabalina A., Lapin I., Goncharova D. Metal Oxide Nanoparticle Preparation by Pulsed Laser Ablation of Metallic Targets in Liquid // Chapter 11 In Book Applications of Laser Ablation - Thin Film Deposition, Nanomaterial Synthesis and Surface Modification, Ed. by Yang D. – Chroatia: InTech, 2016, 426 p.

[10] Adriana Zaleska Doped-TiO2: A Review Recent Patents on Engineering 2008, 2, 157-164

[11] Lapin I.N., Svetlichnyi V.A. Features of the synthesis of nanocolloid oxides by laser ablation of bulk metal targets in solutions // Proc. of SPIE. – 2015. – V. 9810. pp 1–7.

[12] Lopez R., Gomez R., Band-gap energy estimation from diffuse reflectance measurements on sol–gel and commercial TiO_2: a comparative study// J. Sol-Gel Sci. Technol., 2012. V.61. pp. 1-7.

[13] Li W., Ni C., Lin H., Huang C.P., Shah S.I. Size dependence of thermal stability of TiO_2 nanoparticles // J. Appl. Phys., 2004. V. 96. pp. 6662-6668.

[14] Hu Y., Tsai H.-L., Huang C.-L. Effect of brookite phase on the anatase–rutile transition in titania nanoparticles J. Eur. Ceram. Soc., 2003. V. 23. pp. 691-696.

[15] Gotic M., Ivanda M., Popovic S., Music S., Sekulic A., Turkovic A., Furic K. Raman investigation of nanosized TiO_2 // J. Raman Spectrosc., 1997. V. 28. pp 555-558.

[16] Golubovic A., Scepanovic M., Kremenovic A., Askrabic S., Berec V., Dohcevic-Mitrovic Z., Popovic Z.V. Raman study of the variation in anatase structure of TiO_2 nanopowders due to the changes of sol–gel synthesis conditions //J. Sol-Gel Sci. Technol., 2009. V. 49. pp. 311-319.

[17] Mazza T., Barborini E., Piseri P., Milani P. Raman spectroscopy characterization of TiO_2 rutile nanocrystals // Phys. Rev., 2007. V. 75. pp. 045416-045421.

[18] Lukacevic I., Gupta S.K., Jha P.K., Kirin D. Lattice dynamics and Raman spectrum of rutile TiO_2: The role of soft phonon modes in pressure induced phase transition // Mater. Chem. Phys., 2012. V. 137. pp. 282-289.

[19] Chang H., Huang P.J. Thermo-Raman studies on anatase and rutile // J. Raman Spectrosc., 1998. V. 29. pp. 97-102.

[20] Llansola-Portoles M.J., Bergkamp J.J., Finkelstein-Shapiro D., Sherman B.D., Kodis G., Dimitrijevic N.M., Gust D., Moore T.A., Moore A.L. Controlling surface defects and photophysics in TiO_2 nanoparticles // J. Phys. Chem. A, 2014. V. 118. pp. 10631-10638.

[21] Xiang X., Shi X.-Y., Gao X.-L., Ji F., Wang Y.-J., Liu C.-M., Zu X.-T. Effect of N-doping on absorption and luminescence of anatase TiO_2 films // Chin. Phys. Lett., 2012. V. 29. pp. 027801-027804.

[22] Serpone N., Emeline A.V., Kuznetsov V.N., Ryabchuk V.K. Second Generation Visible-Light-Active Photocatalysts: Preparation, Optical Properties, and Consequences of Dopants on the Band Gap Energy of TiO_2 // Chapter 3 In Book Environmentally Benign Photocatalysts, Ed. by Anpo M. Kamat P.V. – Canada: Nanostructure Science and Nanotechnology, 2010, p. 757.

[23] Choudhury B., Choudhury A. Tailoring luminescence properties of TiO_2 nanoparticlesby Mn doping // J. Lumin., 2013. V. 136. pp. 339-346.

Elena D. Fakhrutdinova born in Tomsk in Desember 22, 1987. Received the M.S. degree (2011) in chemistry and PhD degree (2015) at Tomsk State University (TSU). Junior researcher of Laboratory of advanced materials and technologies of the Siberian Physical-Technical Institute of TSU. Her current research interests include synthesis of functional nanomaterials, photocatalysis, pulsed laser ablation, Uv-vis spectroscopy and photoluminescence.

Antonina V. Palatova born on August 2, 1993. In 2017 she received the M.S. degree in physics from the physics faculty at Tomsk State University (TSU). She is getting PhD in physics at Optics and spectroscopy department at TSU. She is currently with the Laboratory of advanced materials and technologies at Siberian Physical-Technical Institute of TSU. Her current research interests include photocatalysis, nanomaterials, pulsed laser ablation.

Valery A. Svetlichnyi born on June 22, 1970; received the M.S. degree (1997) in optics engineering from Tomsk State University; PhD (2001), associate professor (2004), Head of Laboratory of advanced materials and technologies of the Siberian Physical-Technical Institute of TSU (http:amtlab.ru/) He published over 150 scientific publications. His current research is focused on laser techniques and spectroscopic metods for the study of different materials: nanomaterials, semiconductor crystals, dyes. E-mail:v-svetlichnyi@bk.ru